N 72- 28288

NASA TECHNICAL MEMORANDUM

NASA TM X-68107

NASA TM X-68107

CASE FILE COPY

CHOKED FLOW OF FLUID NITROGEN WITH EMPHASIS ON THE THERMODYNAMIC CRITICAL REGION

by R. C. Hendricks, R. J. Simoneau, and R. C. Ehlers
Lewis Research Center
Cleveland, Ohio

TECHNICAL PAPER proposed for presentation at
Cryogenic Engineering Conference
Boulder, Colorado, August 9-11, 1972

CHOKED FLOW OF FLUID NITROGEN WITH EMPHASIS ON THE THERMODYNAMIC CRITICAL REGION

by R. C. Hendricks, R. J. Simoneau, and R. C. Ehlers

National Aeronatuics and Space Administration
Lewis Research Center
Cleveland, Ohio

E-7044

ABSTRACT

Experimental measurements of critical flow rate and pressure ratio for nitrogen flowing through a nozzle are presented. Data for selected stagnation isotherms from 87.5 to 234 K with pressures to 9.3 MN/m^2 are compared to an equilibrium model with real fluid properties and also a nonequilibrium model.

Critical flow pressure ratio along an isotherm tends to peak while the flow rate indicates an inflection. The point is closely associated with the transposed critical temperature and represents a change in the fluid structure.

INTRODUCTION

The critical discharge of fluids is of interest in a variety of industries: transportation, nuclear power, desalinization, aeronautics and space to cite a few. The interest stems primarily from venting requirements and flow measurements, but includes such novel techniques as the production of hydrogen.

The need of adequate theory and data to properly estimate two-phase critical discharge rates has long been recognized by the nuclear power industry and currently a large effort is underway to analyze the events associated with the various types of failures of pressurized water reactors.

Unfortunately the need for accurate venting information is usually not recognized until there is a large scale (costly) accident. For example, the failure of the Apollo 13 fuel cell LOX tank heater and subsequent failure of the venting system caused a mission abort. Other examples are numerous; however one in the mundane of the transportation industry is noteworthy. On June 21, 1970, the derailment of 12 tank cars, each loaded with 30 000 gal of LPG, and subsequent failure of the inadequate venting system led to a holocaust of destruction which will not be readily forgotten by the residents of Crescent City, Illinois.

Reactor safety work has produced a substantial backlog of low reduced pressure ($P/P_{crit} << 1$) critical discharge results for water and alkali metals. Surveys of the two-phase critical discharge have been recently made by Henry and Fauske (1) and Hsu (2). Furthermore much single phase (gas) work considering the effects of compressibility has been completed by Johnson (3). However little data have been accumulated for cryogens discharging through converging nozzles and only the results of Hesson and Peck (4) and Simoneau, Henry, Hendricks and Watterson (5) engage the troublesome near-critical thermodynamic fluid state. Hesson and Peck (4) carried out a detailed study on critical flow of carbon dioxide through nozzle and orifices from the triple point to the thermodynamic critical point. They found that expansions from the saturated liquid state behaved as though no evaporation occurred ahead of the throat (i.e., no quality generated). Also, expansions from the saturated vapor state behaved as though no condensing occurred (i.e., entered the metastable supersaturated state). It is difficult to assess the nature of critical flow rate curve which Hesson and Peck (4) present for the saturated liquid. It would appear that perhaps some of these data may be slightly subcooled, which would have a pronounced increase in the critical flow rate. Henry and Fauske, ref. 6, compare their work to ref. 4, however make no critical comment on the disagreement.

Simoneau et al. (5) completed an extensive test using fluid nitrogen. The nozzle inlet conditions ranged from the highly subcooled liquid ($P_o \approx 4.3$ MN/m^2, $T_o = 90^\circ$ K) to stagnation conditions very near the thermodynamic critical point ($P_c = 3.42$ MN/m^2, $T_c = 126.3^\circ$ K). The highly subcooled data, see figure 1, are in reasonable agreement with the nonequilibrium model of Henry and Fauske (6); however those data for stagnation conditions approaching the thermodynamic critical point depart significantly from the nonequilibrium theory. Compare the 120° and 125° K isotherms with the data for both critical flow rate and critical flow pressure ratio, figs. 1(a) and (b).

The data taken thus far represent the first step in defining the nature of critical flow through nozzles for a fluid near its thermodynamic critical point. However in order to determine a critical flow rate map for a fluid, data must include nozzle throat conditions approaching the thermodynamic critical point as well as stagnation temperatures ranging from the boiling point to near ambient, and pressures ranging up to several times critical pressure. The primary objective of this paper will be to present critical flow data for nitrogen over the range of nozzle stagnation conditions $0.7 < T_o/T_c < 2$; $0.35 < P_o/P_c < 3$. The secondary objectives will be to compare the data to nonequilibrium and equilibrium theories.

APPARATUS, INSTRUMENTATION, AND OPERATIONS

The essential features of the test apparatus are shown in figure 2 and is essentially the same as that used in ref. 5. The stagnation chamber was a large volume properly baffled to avoid jetting. The test nozzle was an axisymmetric venturi flowmeter which was adapted for use in this experiment. The nozzle was instrumented with nine pressure taps as shown in figure 2. The stagnation temperature was measured with two platinum resistance thermometers. Flow rates were metered with a venturi flowmeter in the high pressure storage dewar and monitored by an orifice flowmeter in the low pressure gaseous stream downstream of the heat exchanger.

The test section assembly was wrapped with fiberglas insulation and placed in the vacuum chamber of a cryogenic blowdown facility. The blowdown system could operate for about 5 minutes at the maximum flow rate of the present test. Liquid nitrogen could be delivered to the stagnation chamber at the desired pressure up to 9.5 MN/m^2 and temperatures from 88° to 279° K.

The data were recorded electronically and reduced using a high speed data acquisition system with recording accuracy better than 0.1%. The static pressure transducers were better than 1/2% of full scale and would zero-flow-calibrate to better than 1/4% of full scale. The real test for accuracy was however based on the flowmeter. No data were taken unless the pre-run system checks indicated that the venturi and orifice flowmeters agreed within 1%. Redundant temperature measurements were usually within $\pm 0.1^\circ$ K, with absolute accuracy to within ±1/2%.

In acquiring data, the bulk fluid in the high pressure storage dewar was raised to the desired temperature level, usually under 3.4 MN/m^2 pressure. The dewar was then pressurized and data points taken at the desired stagnation pressures. These data were then tabulated and families of isotherms were selected from them and are presented as Table I.

When discussing accuracy a word of caution should be interjected. In two-phase critical flow the precise location of the physical throat is difficult to determine. Thus, although the pressure measurement is accurate, it may not be the true throat pressure. No estimate can be given for potential error but we do know the measured P_t yields excellent single phase values.

DISCUSSION OF RESULTS

Flow Rate and Pressure Ratio Data

The data for the critical (choked) flow rate and for the critical flow pressure ratio* P_t/P_o of nitrogen flowing through a nozzle for

---

*The use of the word "critical," especially in connection with pressure ratio can be the source of confusion in the present work. The "critical pressure ratio" P/P_c is the ratio of any pressure P to the thermodynamic critical pressure P_c. The "critical flow pressure ratio" is the ratio of the throat pressure P_t, at which the flow rate is a maximum, to the stagnation pressure P_o for that flow.

selected stagnation isotherms are found in Table I and plotted as a function of stagnation pressure in figures 3 and 4. Figures 3 and 4 are broken down into parts (a), (b), and (c) primarily because some of the isotherms are grouped quite closely together and subdividing the figures makes them easier to read. The stagnation temperature was varied from 87.5° to 234° K but not in uniform increments. These data may be cross-plotted and then replotted with regular isotherm increments; however this represents a double smoothing of the data and will be discussed later. Since the change in critical flow rate for a 1° K change in stagnation temperature (fixed stagnation pressure) is readily detectable, many isotherms near the thermodynamic critical temperature are plotted. These isotherms tend to merge near the critical pressure, P_c.

There are several trends in the data plots that are worthy of note. One of the more complete isotherms is at 130.4° K and indicates an inflection point near 4.3 MN/m^2 (fig. 3(a)). This inflection point corresponds to a rapid change and peak in the critical flow pressure ratio P_t/P_o as shown in figure 4(a). This appears to be closely related to a change in fluid structure at the transposed critical temperature (temperature at which Cp peaks (see also ref. 14)). The transposed critical temperature at 4.35 MN/m^2 is about 131.6° K which is quite close to the inflection point and peak point noted in figures 3(a) and 4(a), respectively. Similar peaking and inflection points are noted for the several near critical temperature isotherms at 1° K intervals (figs. 3(c) and 4(c)).

As previously mentioned, the data of figures 3 and 4 may be cross-plotted along isobars rather than isotherms as illustrated in figure 5. This represents a smoothing of the data but should be a good representation of an experiment run along isobars. In many cases, figure 5 may be of greater utility than figure 3. Figure 5 may again be cross-plotted to give regular isothermal increments. This would represent a double smoothing of the data, which can be dangerous especially where sharp changes are occurring. As a check the 96.4° K isotherm of figure 3(a) was obtained from figure 5 and found to agree within 0.6%.

The transposed critical temperature, T^*, locus is shown on figure 5, and as has been pointed out above the point of inflection in the flow rate curve is near T^*.

In the introduction it was mentioned that throat pressures near critical should be obtained to complete the flow map. Table I contains points with throat pressure near the critical pressure. No significant differences were found relative to the other pressure along the saturation locus. This can be seen in the data of Table II. In the first set the throat pressure P_t is near the thermodynamic critical pressure (P_c = 3.42 MN/m^2) and the stagnation entropy S_o is near the critical entropy (S_c = 1.813 joule/gm °K). In the second set of data the throat pressure is slightly below critical pressure and in the third set it is substantially below critical pressure. In each set the measured throat pressure was 0.1 to 0.3 MN/m^2 below the saturation pressure which corresponds to the stagnation entropy $P_{sat}(S_o)$. Care must be exercised in commenting on the actual numbers since the location of the physical throat is difficult to establish; however, the qualitative observation that the $P_{sat} - P_t$ difference is not particularly sensitive to the proximity of the thermodynamic critical point is worthy of note.

Theoretical Models

The range of the present experiment is such that the expansion in the nozzle could be all single phase for some conditions and could be two-phase for other conditions. Accordingly the selection of theoretical models and computational procedures may change from region to region of the experiment.

In this paper two theoretical models which are popular in choked flow will be examined. The first of these is an equilibrium isentropic expansion. The second is a nonequilibrium expansion which attempts to account for the rate of change of the key variables. Both models begin with the same equations. The basic equations are presented in the Appendix. In both cases the phase velocities are assumed equal (i.e., k = 1). Thus the basic flow equation is (A9):

$$G^2 = -\frac{2}{v^2} \int_{P_o}^{P} v \, dP \qquad (1)$$

where

$$v = xv_g + (1 - x)v_\ell \qquad (2)$$

The critical flow rate, based on the condition that $\frac{dG}{dP} = 0$, is equation (A14)

$$G^2_{max} = -\left[x \frac{dv_g}{dP} + (1 - x) \frac{dv_\ell}{dP} + (v_g - v_\ell) \frac{dx}{dP}\right]_t^{-1} \qquad (3)$$

Equilibrium Model

The equilibrium calculations were carried out by iteratively maximizing equation (1). Other equilibrium methods are available, Moody (9) for example. This merely seems the most direct and easiest way of handling the thermodynamic critical region. Throughout the expansion the properties are assumed to be in thermodynamic equilibrium at the local pressure and stagnation entropy. The equilibrium properties were obtained from a property package entitled Subroutine GASP (11), which was based on an equation of state for nitrogen by Bender (12) and earlier work of Strobridge (13). The property program is quite elaborate and among the available combinations of independent variables are pressure and entropy which is most useful in an isentropic expansion. While computations of this nature have been carried out before, they frequently assume ideal gas properties and have not been done for the dense gas region around the critical point which is the focus of the present experiment. It should be pointed out that, while the expansion begins in the single phase region, the majority of the cases wind up two-phase at the throat.

When the expansion enters the two-phase region, which is frequently the case, the computation can be checked with equation (3). Care must be exercised in dealing with the subcooled liquid region since equation (1) does not cross the saturated liquid boundary smoothly and if the critical low throat pressure is near saturation the function may not maximize properly. Equilibrium calculations will not be presented for the subcooled liquid region partly because of this maximization question and partly because the work of Henry and Fauske (6) indicates that the nonequilibrium model is more correct for subcooled liquids. Equilibrium calculations will however be presented for the vapor region.

Nonequilibrium Model

The model proposed by Henry and Fauske (6) attempts to account for the high degree of nonequilibrium which may accompany an expansion from a liquid or low quality stagnation condition to two-phase at the throat. The model implies that for very short nozzle residence times the interphase heat and mass transferred may be negligible but the rates of heat and mass transfer may be substantial. Thus all the physical properties may not stay in thermodynamic equilibrium. Computations based on this model were presented earlier in the paper by Simoneau et al. (5). In addition to the no slip assumption, reference 5 also assumed $x_t \approx 0$ and $dv_\ell/dP \approx 0$. In addition an empirical formulation for the rate of mass transfer proposed by Henry (5) was also used:

$$\left.\frac{dx}{dP}\right]_t = -\left[\frac{N}{(S_g - S_\ell)}\frac{dS_\ell}{dP}\right]_{t,E} \tag{4}$$

where $N = x_E/0.14$. Under these assumptions equation (3) becomes

$$G^2_{max} = \left[\frac{N(v_g - v_\ell)}{(S_g - S_\ell)}\frac{dS_\ell}{dP}\right]^{-1}_{t,E} \tag{5}$$

On the vapor side the dx/dP contribution becomes smaller and of course x_t is closer to 1, thus the nonequilibrium effects are substantially reduced and the two models tend to merge. Equation (5) was solved iteratively by means of a computer program supplied by Henry (14). The program used the saturation properties published by Strobridge (13), and in the liquid region assumed the density was constant at the saturation value corresponding to the stagnation temperature.

Comparison of Data and Theory

The results of the calculations are shown along with the data in figures 6(a) and (b). Examining first the critical flow rate data (fig. 6(a)) we see that in the subcooled liquid region the additional data continue the trends established in reference 5 (fig. 1 herein). Between 90° and 120° K the nonequilibrium theory follows the slope of the data quite well and predicts the flow rates to within 5 to 15% over the whole range. One result that needs further study is that the 90° K data are below theory while the 120° K data are above theory, thus the 5 to 15% deviation is systematic rather than random. Generally in this experiment it was not possible to obtain stagnation pressures very near saturation; however, along the 120° K isotherm the last point is quite close. The trend of convergence to the nonequilibrium line in contrast to the equilibrium line encourages use of the nonequilibrium theory for saturated liquid nitrogen. The critical flow pressure ratio results (fig. 6(b)) in the subcooled region are less encouraging. For the 90° and 100° K isotherms the agreement with theory is quite good. Beyond this toward 120° K the disagreement becomes substantial. A question concerning two-dimensional effects in the nozzle was raised in reference 5. Since the same nozzle was used herein, this deviation remains unresolved.

Much of the new data presented herein were taken along isotherms at or above the critical isotherm with stagnation pressures from near the thermodynamic critical pressure to values high enough to produce throat pressures near the critical point. The results are compared to the isentropic equilibrium expansion calculations in figures 6(a) and (b). In general, the agreement between theory and data is very good in both critical flow rates and critical flow pressure ratios. It is particularly encouraging that the theory predicts the peaking in the pressure ratio data.

The area between 110° and 130° K at present remains unresolved. Data acquired with a different nozzle will be required to establish trends for further analysis.

CONCLUSIONS

A critical flow experiment was performed with fluid nitrogen in a converging-diverging nozzle at stagnation conditions from 87.5° to 234° K and pressures to 9.3 MN/m^2, with particular emphasis on the thermodynamic critical region. The nozzle throat conditions ranged from two-phase to near-critical to gaseous. The following conclusions can be drawn:

1. Proximity of the fluid in the stagnation chamber to the critical Point causes a significant influence on the critical flow rate and pressure ratio curves. The flow rate exhibits an inflection and the pressure

ratio a sharp peak when stagnation conditions are near the transposed critical point.

2. At stagnation temperatures above the thermodynamic critical temperature (126.3° K) the critical flow rates and critical flow pressure ratios can be predicted quite satisfactorily by an isentropic equilibrium expansion. For subcooled and saturated liquids (90° to 110° K) nonequilibrium effects appear significant and the analysis of Henry and Fauske (7) is suggested. Between 110° and 130° K for subcooled liquids the data and theory trends are not consistent and further investigation is required.

3. Data were acquired for nozzle throat conditions approaching the thermodynamic critical point; however no anomalous behavior was observed.

SYMBOLS

A	area, cm^2
C_p	specific heat at constant pressure, joule/gm °K
G	mass flow rate/unit area, gm/cm^2-sec
$K = \frac{u_g}{u_\ell}$	slip ratio
$N = \frac{x_E}{0.14}$	empirical factor (rate of mass transfer)
P	pressure, MN/m^2
s	entropy, joule/gm-°K
T	temperature, °K
u	velocity, cm/sec
v	specific volume, cm^3/gm
w	mass flow rate, gm/sec
x	quality

Subscripts:

c	thermodynamic critical
E	equilibrium

g	gas (vapor)
ℓ	liquid
m	interphase momentum weighted
max	maximum
o	stagnation
r	reduced
t	throat

APPENDIX - BASIC TWO-PHASE CRITICAL FLOW EQUATIONS

The two-phase critical flow equations occur frequently in the literature and the derivation will not be repeated herein; however, a few key steps will be pointed out. The work of Fauske (7) is a good source for the details of the derivation. The one-dimensional momentum equation in the absence of friction is:

$$-A\ dP = d(u_\ell W_\ell + u_g W_g) \tag{A1}$$

Using the basic definitions:

$$G = \frac{W}{A};\ x = \frac{W_g}{W},\ \text{and}\ (1 - x) = \frac{W_\ell}{W} \tag{A2}$$

and one-dimensional continuity (W = constant), equation (A1) can be rewritten as

$$-\frac{1}{G} = \frac{d}{dP}\,[xu_g + (1 - x)u_\ell] \tag{A3}$$

Introducing the definition of slip ratio:

$$K = \frac{u_g}{u_\ell} \tag{A4}$$

and employing the basic definition $A_g = A - A_\ell$ as well as those in (A2) it can be shown that

$$u_\ell = \frac{xv_g + (1 - x)Kv_\ell}{KG} \tag{A5}$$

Equations (A4) and (A5) can be used in equation (A3) to yield:

$$-1 = G\,\frac{d}{dP}\,(v_m G) \tag{A6}$$

where

$$v_m = \left[\frac{xK + (1 - x)}{K}\right][xv_g + K(1 - x)v_\ell] \tag{A7}$$

When $x = 0$ or 1, v_m represents single phase liquid and gas, respectively, while $K = 1$, the no slip condition, implies the flow is homogeneous. Fauske (7) points out that the specific volume v_m in equation (A7) accounts for the momentum exchange between phases. Equation (A6) can be written:

$$-v_m = v_m G \frac{d}{dP} (v_m G) = \frac{1}{2} \frac{d}{dP} (v_m G)^2 \tag{A8}$$

Equation (A8) can be integrated over the length of the nozzle, subject to the condition $G = 0$ at $P = P_o$ to yield:

$$G^2 = - \frac{2}{v_m^2} \int_{P_o}^{P} v_m \, dP \tag{A9}$$

Equation (A9) is evaluated along an isentropic path and G_{max} can be determined iteratively. The maximum could be determined by carrying out the differentiation indicated in equation (A8) and setting $dG/dP = 0$; however, the solution for the maximum would still be iterative. Carrying out the differentiation in equation (A6) yields

$$-1 = G\left[v_m \frac{dG}{dP} + G \frac{dv_m}{dP}\right] \tag{A10}$$

The critical flow condition says that $dG/dP)_t = 0$ and equation (A10) becomes

$$G_{max}^2 = - \frac{dv_m}{dP}\Bigg]_t^{-1} \tag{A11}$$

Carrying out the differentiation yields:

$$\begin{aligned} G_{max}^2 = -\Bigg[K\Bigg\{x[1 + x(K - 1)] \frac{dv_g}{dP} + K[1 + x(K - 2) - x^2(K - 1)] \frac{dv_\ell}{dP} \\ + x(1 - x)\left(Kv_\ell - \frac{v_g}{K}\right) \frac{dK}{dP} \\ + v_g[1 + 2x(K - 1)] + Kv_\ell[2(x - 1) + K(1 - 2x)] \frac{dx}{dP}\Bigg\}^{-1}\Bigg]_t \end{aligned} \tag{A12}$$

In this paper we shall assume $K = 1$ (no slip condition) and equation (A7) becomes:

$$v_m\Big]_{K=1} = v = xv_g + (1 - x)v_\ell \tag{A13}$$

In this case equation (A13) will be used in evaluating the integral, equation (A9), instead of equation (A7). Similarly equation (A12) becomes:

$$G_{max}^2 = -\left[x \frac{dv_g}{dP} + (1 - x) \frac{dv_\ell}{dP} + (v_g - v_\ell) \frac{dx}{dP}\right]_t^{-1} \tag{A14}$$

TABLE I. - CRITICAL DISCHARGE DATA FOR NITROGEN

FLOWING THROUGH A NOZZLE

Run	P_o, MN/m^2	T_o, K	G, gm/cm^2-sec	$Pr = P_t/P_o$	Remarks
			T = 116.7±0.4		
944	2.064	117.0	891	0.5885	
827	2.050	116.3	3037	.5312	
645	7.676	116.9	8087	.1914	
644	6.312	116.7	7078	.2436	
643	4.861	116.7	5818	.3224	
642	3.381	116.6	4615	.3241	
517	8.363	117.2	8350	.1875	
856	2.097	117.3	1446	.6317	
			T = 106.5±0.1		
699	8.268	106.6	9334	0.1088	
500	3.472	106.5	5490	.277	
502	4.817	106.4	6850	.188	
			T = 119.6±0.3		
529	6.985	119.7	7390	0.247	
528	5.608	119.5	6260	.314	
526	2.667	119.9	2010	.665	
527	4.083	119.3	4970	.340	
851	5.356	119.6	6009	.3236	
852	4.375	119.9	5127	.3407	
853	3.398	119.7	4294	.4184	
854	2.863	119.8	3423	.5797	
647	5.942	119.3	6484	.2921	
813	2.305	119.0	1002	0.5634	Indicator*
530	8.084	120.6	8060	.2139	Indicator*
			T = 121.2±0.2		
936	2.540	121.0	1298	0.5747	
862	3.768	121.2	4359	.4405	
863	2.926	121.4	2911	.6996	
865	2.550	121.1	1714	.6302	
533	5.508	121.2	5990	.334	
534	4.794	121.2	5350	.351	
535	4.136	121.2	4770	.382	
536	3.532	121.4	4000	.504	

TABLE I. - Continued. CRITICAL DISCHARGE DATA FOR

NITROGEN FLOWING THROUGH A NOZZLE

Run	P_o, MN/m^2	T_o, K	G, gm/cm^2-sec	$Pr = P_t/P_o$	Remarks
			$T = 87.5 \pm 0.1$		
907	7.637	87.6	10 060	0.03476	
449	8.474	87.4	10 610	.0306	
457	5.527	87.5	8 500	.0457	
464	7.068	87.6	9 670	.0366	
			$T = 90.5^{+0.1}_{-0.2}$		
452	6.224	90.5	8 940	0.051	
466	4.653	90.6	7 650	.068	
459	3.432	90.3	6 500	.090	
			$T = 96.4^{+0.4}_{-0.1}$		
462	1.465	96.8	3 550	0.359	
485	4.237	96.4	7 050	.1078	
490	4.987	96.4	7 650	.10	
741	6.716	96.4	8 943	.0711	
735	4.234	96.4	6 948	.1141	
876	2.795	96.3	5 501	.1770	
841	1.732	96.4	4 052	.2993	
			$T = 103.2$		
802	7.744	103.2	9 244	0.0896	
801	6.111	103.2	8 067	.1156	
786	3.513	103.2	5 748	.2144	
790	6.031	103.2	8 016	.1168	
797	3.649	103.2	5 904	.2054	
			$T = 111.2 \pm 0.7$		
857	1.544	111.4	990	0.5976	May be two-phase
897	1.45	110.5	712	.601	May be two-phase
858	1.506	110.8	978	.6083	May be two-phase
833	1.47	110.8	825	.6058	May be two-phase
710	4.173	111.8	5 655	.310	
711	4.825	111.8	6 292	.2653	
712	5.599	111.9	6 953	.2228	
638	5.976	111.0	7 324	.1963	
637	4.122	111.8	5 588	.3135	
639	8.171	110.6	8 946	.1329	
512	5.505	110.7	7 000	.217	

TABLE I. - Continued. CRITICAL DISCHARGE DATA FOR

NITROGEN FLOWING THROUGH A NOZZLE

Run	P_o, MN/m^2	T_o, K	G, gm/cm^2-sec	$Pr = P_t/P_o$	Remarks
			$T = 122.0 \pm 0.2$		
540	4.916	122.2	5340	0.359	
539	4.142	121.9	4650	.415	
538	3.358	121.8	3600	.586	
537	2.941	122.1	2625	.758	
442	6.974	122.3	7060	0.27	Indicator*
			$T = 124.4^{+0}_{-0.2}$		
544	7.994	124.4	7600	0.252	
545	6.916	124.4	6770	.299	
546	6.197	124.4	6200	.337	
547	5.480	124.4	5550	.367	
548	4.960	124.4	5070	.402	
549	4.187	124.2	4200	.52	
550	3.496	124.3	2990	.719	
			$T = 125.1 \pm 0.2$		
935	3.121	125.2	1645	0.5844	
553	4.244	125.0	4100	.5480	
569	3.461	125.0	2570	0.785	
568	4.186	124.9	4005	.556	
567	4.858	125.0	4850	.437	
566	6.238	125.3	6120	.341	
565	7.604	125.3	7190	.273	
564	8.803	125.1	8100	.224	
			$T = 126.0 \pm 0.2$		
436	6.22	125.9	6040	0.347	
437	5.615	126.1	5480	.420	
577	8.631	126.2	7860	.240	
581	4.895	126.0	4710	.470	
582	4.179	125.8	3785	.600	
584	3.526	125.9	2390	.670	
597	6.884	126.2	6540	.318	
596	8.396	126.2	7670	.250	
598	5.550	126.0	5390	.392	
599	4.220	125.8	3830	.595	
600	3.770	126.1	7440	.755	
603	8.537	125.8	7850	.240	
604	6.899	126.0	6560	.315	
605	5.631	125.8	5510	.3805	

TABLE I. - Continued. CRITICAL DISCHARGE DATA FOR

NITROGEN FLOWING THROUGH A NOZZLE

Run	P_o, MN/m^2	T_o, K	G, gm/cm^2-sec	$Pr = P_t/P_o$	Remarks
			$T = 127.2^{+0.2}_{-0.1}$		
608	8.348	127.4	7494	0.2608	
609	6.892	124.4	6372	.3312	
610	5.522	127.1	5190	.423	
611	4.157	127.2	3320	.68	
612	3.846	127.4	2582	.78	
			$T = 126.9 \pm 0.1$		
571	8.864	126.8	7930	0.236	
572	7.633	127.0	7000	.289	
573	6.288	127.0	5920	.362	
574	4.933	126.9	4560	.497	
575	3.817	126.9	2690	.775	
			$T = 130.4 \pm 0.3$		
757	4.425	130.2	3006	0.7263	
770	5.169	130.3	4213	.5692	
899	4.183	130.7	2426	.6276	
894	4.084	130.5	2322	.6190	
622	5.577	130.4	4630	.5082	
624	4.336	130.1	2804	.7419	
884	5.509	130.3	4591	.5157	
679	4.923	130.6	3731	.6251	
680	4.535	130.1	3200	.6958	
682	4.501	130.2	3127	.7074	
687	4.344	130.7	2697	.7073	
621	6.981	130.9	5963	0.3732	Indicators*
945	3.749	130.9	1730	.6135	Indicators*
620	8.529	131.1	7183	.2880	Indicators*
			$T = 133.8 \pm 0.1$		
807	8.359	133.7	6652	0.3243	
759	6.573	133.9	5185	.4588	
754	8.348	133.8	6788	.3273	
661	4.760	133.8	2786	.6979	
662	4.733	133.7	2753	.7011	

TABLE I. - Continued. CRITICAL DISCHARGE DATA FOR

NITROGEN FLOWING THROUGH A NOZZLE

Run	P_o, MN/m^2	T_o, K	G, gm/cm^2-sec	$Pr = P_t/P_o$	Remarks
			T = 139.5±0.3		
938	8.557	139.3	6050	0.3681	
911	9.098	139.4	6464	.3406	
656	8.470	139.8	5871	.3771	
669	5.263	139.8	2673	.6024	
668	5.863	139.3	3403	.5669	
923	7.689	139.9	5245	.4238	
904	9.270	140.3	6472	.3392	Indicators*
657	7.563	139.1	5208	.4280	
			T = 156±2		
947	9.403	157.8	4472	0.4235	
729	6.564	158.4	2659	.4864	Indicator*
751	6.946	155.1	3080	.4765	
670	8.603	154.4	4099	.4339	
671	6.833	156.3	2851	.4808	
948	7.464	153.8	3493	.4623	Indicator*
			T = 176.9±1.6		
690	9.024	178.5	3191	0.4719	
691	6.857	176.8	2325	.4944	
697	5.802	175.0	1946	.500	
672	8.706	175.5	3129	.4746	
506	4.630	179.3	1460	.513	Indicator*
			T = 234.1±1.1		
725	4.699	235.2	1240	0.508	
726	.749	234.7	204	.5957	
747	3.029	233.0	823	.5108	
			T = 131±0.2		
932	4.289	130.9	2565	0.6517	
811	4.386	130.8	2664	.7144	
883	6.902	131.2	5859	.3864	
760	4.518	131.2	2933	.7248	

TABLE I. - Continued. CRITICAL DISCHARGE DATA FOR

NITROGEN FLOWING THROUGH A NOZZLE

Run	P_o, MN/m^2	T_o, K	G, gm/cm^2-sec	$Pr = P_t/P_o$	Remarks
			T = 132±0.2		
768	9.075	132.1	7562	0.2753	
684	5.606	131.9	4388	.5406	
882	8.913	132.0	7358	.2815	
809	5.493	132.0	4159	.5566	
900	4.576	132.2	2798	.7192	
928	4.717	131.8	3118	.6924	
929	4.906	132.2	3344	.6632	
			T = 133±0.2		
685	6.590	133.0	5254	0.4452	
915	4.666	132.9	2808	.7085	
808	6.721	133.0	5539	.4296	
688	5.556	132.8	4151	.5652	
893	4.666	132.8	2920	.7092	
			T = 134±0.2		
759	6.573	133.9	5185	0.4588	
663	4.798	134.1	2796	.6925	
892	5.489	134.2	3817	.5938	
661	4.760	133.8	2786	.6979	
754	8.348	133.8	6788	.3273	
			T = 135±0.2		
664	5.111	135.1	3095	0.6505	
817	4.209	134.8	1912	.6620	
902	5.671	135.2	3882	.5782	
942	4.502	135.2	2245	.6865	
758	8.376	134.8	6651	.338	
			T = 136±0.1		
689	8.505	136.0	6473	0.3434	
922	5.673	136.1	3716	.582	
946	4.188	135.9	1958	.6555	

TABLE I. - Concluded. CRITICAL DISCHARGE DATA FOR

NITROGEN FLOWING THROUGH A NOZZLE

Run	P_o, MN/m^2	T_o, K	G, gm/cm^2-sec	$Pr = P_t/P_o$	Remarks
			T = 138.		
940	5.491	138.0	4521	0.6028	Mass flow (questionable)
912	7.555	138.2	5372	.4216	
658	6.282	138.2	4638	.4794	Mass flow (questionable)
890	9.182	138.2	6711	.3281	
			T = 98.9±0.3		
488	2.114	99.2	4440	0.296	
736	2.454	98.6	4895	.2387	
742	4.819	98.1	7374	0.1117	Indicator*
877	2.065	98.6	4402	.2905	
783	7.862	99.8	9433	.07407	
847	2.082	98.5	4410	.2868	(a)
842	1.381	98.3	3276	0.4197	(a) Indicator*

[a]Oscillations noted.
*Used to indicate data trends.

TABLE II. - RUNS WITH CONSTANT THROAT PRESSURE

Run	P_o, MN/m^2	T_o, ^oK	S_o, j/gm-^oK	P_{sat}, MN/m^2	P_t, MN/m^2	P_t/P_o	G, gm/cm^2-sec	$P_{sat} - P_t$, MN/m^2	S_{tank}, j/gm ^oK	
658	6.282	138.2	1.774	3.420	3.291	0.479	4640	0.129	1.614	
559	6.113	137.1	1.756	3.419	3.298	.540	4060	.121	1.613	
660	5.386	135.5	1.791	3.413	3.318	.616	3420	.095	1.614	P_{tank}
661	4.760	133.8	1.840	3.417	3.321	.698	2790	.096		9.26 MN/m^2
662	4.733	133.7	1.842	3.418	3.318	.701	2750	.100		T_{tank}
663	4.798	134.1	1.847	3.420	3.323	.693	2800	.097		139 ^oK
664	5.111	135.1	1.824	3.407	3.325	.651	3100	.082		
665	6.557	138.7	1.762	3.420	3.315	.506	4280	.105	1.629	
666	8.534	142.0	1.715	3.391	3.301	.387	5600	.090	1.638	
678	5.608	131.4	1.612	3.188	2.962	0.528	4480	0.226	1.465	
679	4.923	130.6	1.645	3.272	3.078	.625	3730	.194	1.464	P_{tank}
680	4.535	130.1	1.677	3.336	3.155	.696	3200	.181	1.464	9.35
681	4.202	129.6	1.721	3.398	3.098	.737	2690	.300	1.465	
682	4.501	130.2	1.688	3.356	3.184	.707	3130	.172		T_{tank}
683	4.843	130.8	1.664	3.312	3.132	.647	3560	.180		131
684	5.606	131.9	1.628	3.231	3.030	.541	4390	.201		
685	6.590	133.0	1.597	3.146	2.934	.445	5250	.212	1.470	
643	4.861	116.7	1.253	1.797	1.567	0.322	5820	0.230	1.092	P_{tank}
644	6.312	116.7	1.225	1.684	1.538	.244	7080	.146	1.097	9.52
645	7.676	116.9	1.207	1.610	1.469	.191	8090	.141	1.105	
646	8.379	117.3	1.204	1.599	1.482	.177	8480	.117	1.120	T_{tank} 113

REFERENCES

1. Henry, R. E.; Grolmes, M. A.; and Fauske, H. K.: Pressure Drop and Compressible Flow of Cryogenic Liquid-Vapor Mixtures. Heat Transfer at Low Temperatures. Walter Frost, ed., Plenum Press, to be published (c 1972).

2. Hsu, Y. Y.: Review of Critical Flow Propagation of Pressure Pulse and Sonic Velocity, to be published as NASA Technical Note.

3. Johnson, Robert C.: Thermodynamic Functions for Calculating the Critical Flow of Methane and Natural Gas Through Nozzles, to be published as NASA Technical Note.

4. Hesson, James C.; and Peck, Ralph E.: Flow of Two-Phase Carbon Dioxide Through Orifices. AIChE J., vol. 4, no. 2, June 1958, pp. 207-210.

5. Simoneau, R. J.; Henry, R. E.; Hendricks, R. C.; and Watterson, R.: Two-Phase Critical Discharge of High Pressure Liquid Nitrogen. Presented at the 13th International Congress of Refrigeration, NAS/NRC, Washington, D.C., Aug. 27-Sept. 3, 1971.

6. Henry, Robert E.; and Fauske, Hans K.: The Two-Phase Critical Flow of One-Component Mixtures in Nozzles, Orifices, and Short Tubes. J. Heat Transfer, vol. 93, no. 2, May 1971, pp. 179-187.

7. Fauske, Hans K.: Contribution to the Theory of Two-Phase, One-Component Critical Flow. Rep. ANL-6633, Argonne National Lab., Oct. 1962.

8. Shapiro, Ascher H.: The Dynamics and Thermodynamics of Compressible Fluid Flow. Ronald Press Co., 1953.

9. Moody, F. J.: Maximum Flow Rate of a Single Component, Two-Phase Mixture. J. Heat Transfer, vol. 87, no. 1, Feb. 1965, pp. 134-142.

10. Levy, S.: Prediction of Two-Phase Critical Flow Rate. J. Heat Transfer, vol. 87, no. 1, Feb. 1965, pp. 53-58.

11. Hendricks, R. C.; Baron, A.; Peller, I.; and Pew, K. J.: GASP - A Computer Code for Calculating the Thermodynamic and Transport Properties for Eight Fluids - Helium, Methane, Neon, Nitrogen, Carbon Monoxide, Oxygen, Argon, Carbon Dioxide. Presented at the 13th International Congress of Refrigeration, NAS/NRC, Washington, D.C., Aug. 27-Sept. 3, 1971.

12. Bender, E.: Equations of State Exactly Representing the Phase Behavior of Pure Substances. Proceedings of the Fifth Symposium on Thermophysical Properties. ASME, 1970, pp. 227-235.

13. Strobridge, Thomas R.: The Thermodynamic Properties of Nitrogen from 64° to 300° K Between 0.1 and 200 Atmospheres. Tech. Note 129, National Bureau of Standards, Jan. 1962.

14. Henry, Robert E.: Private communication.

15. Hendricks, Robert C.; Simoneau, Robert J.; and Smith, Ray V.: Survey of Heat Transfer to Near-Critical Fluids. NASA TN D-5886, 1970.

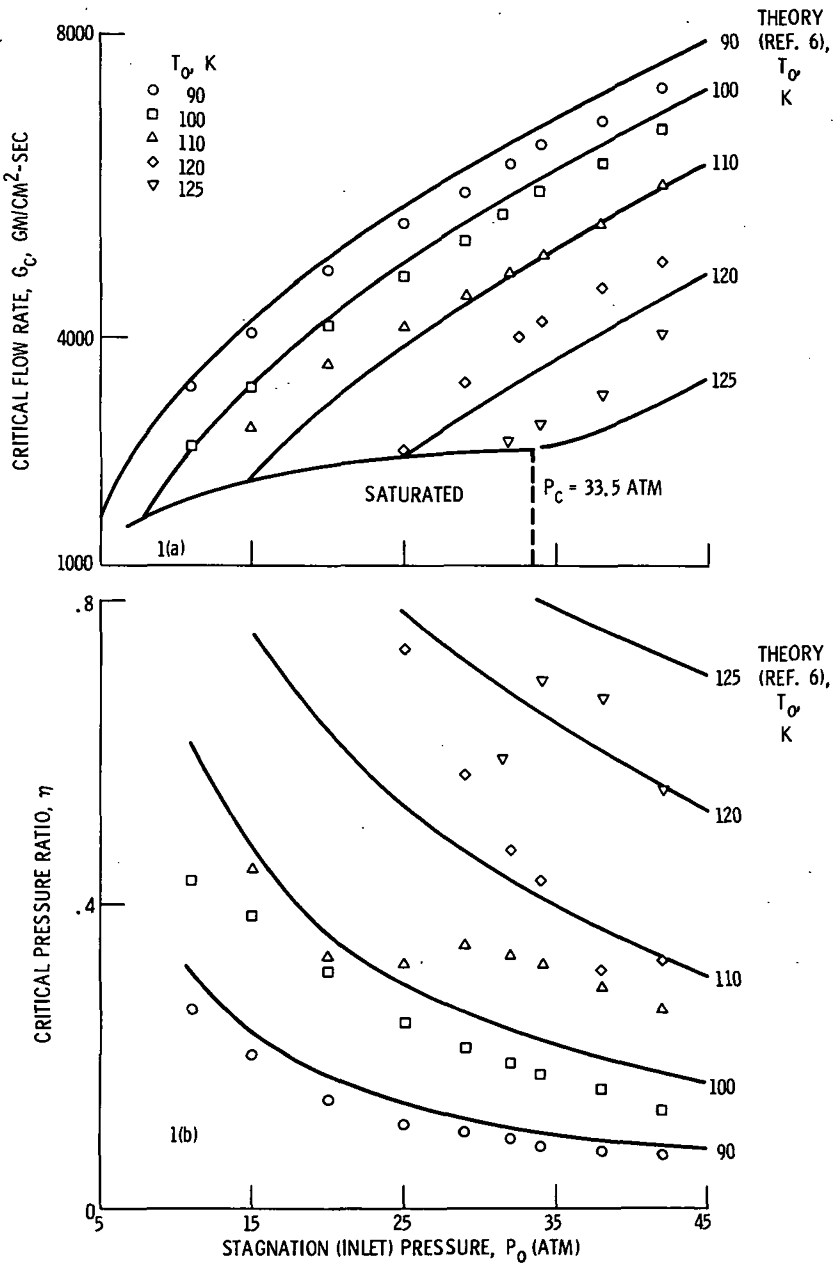

Figure 1. - Critical flowrate and pressure ratio of nitrogen (ref. 5).

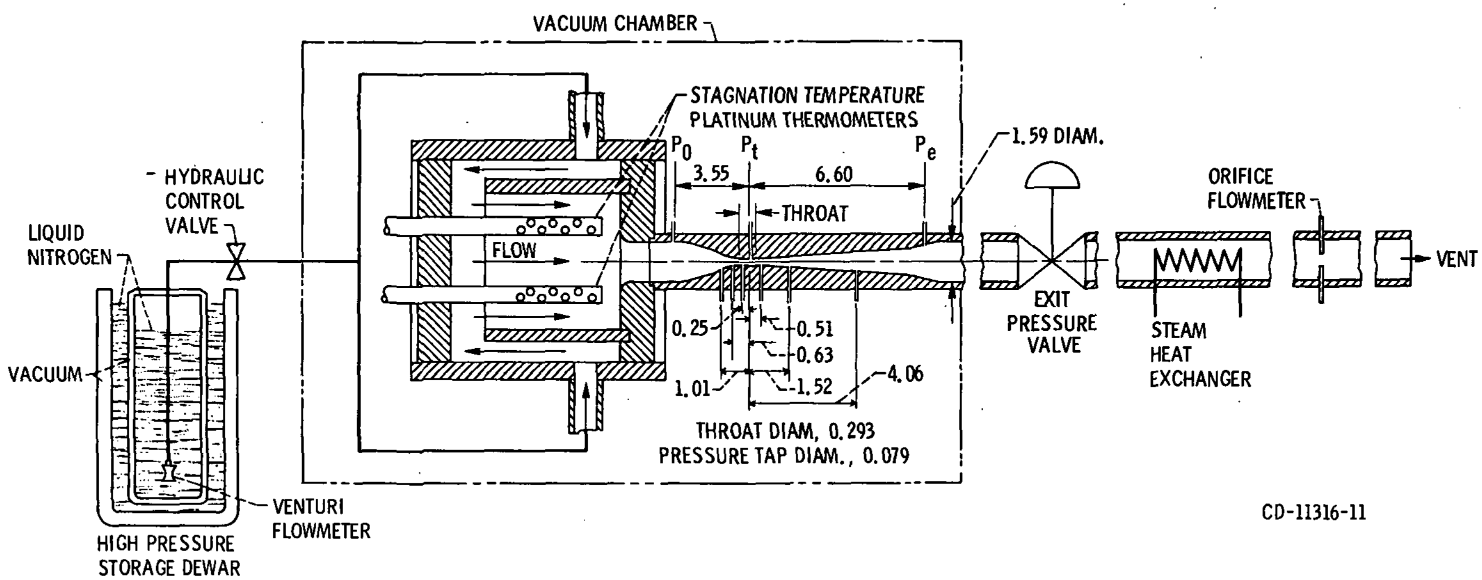

Figure 2. - Test section assembly. (All dimensions in cm.)

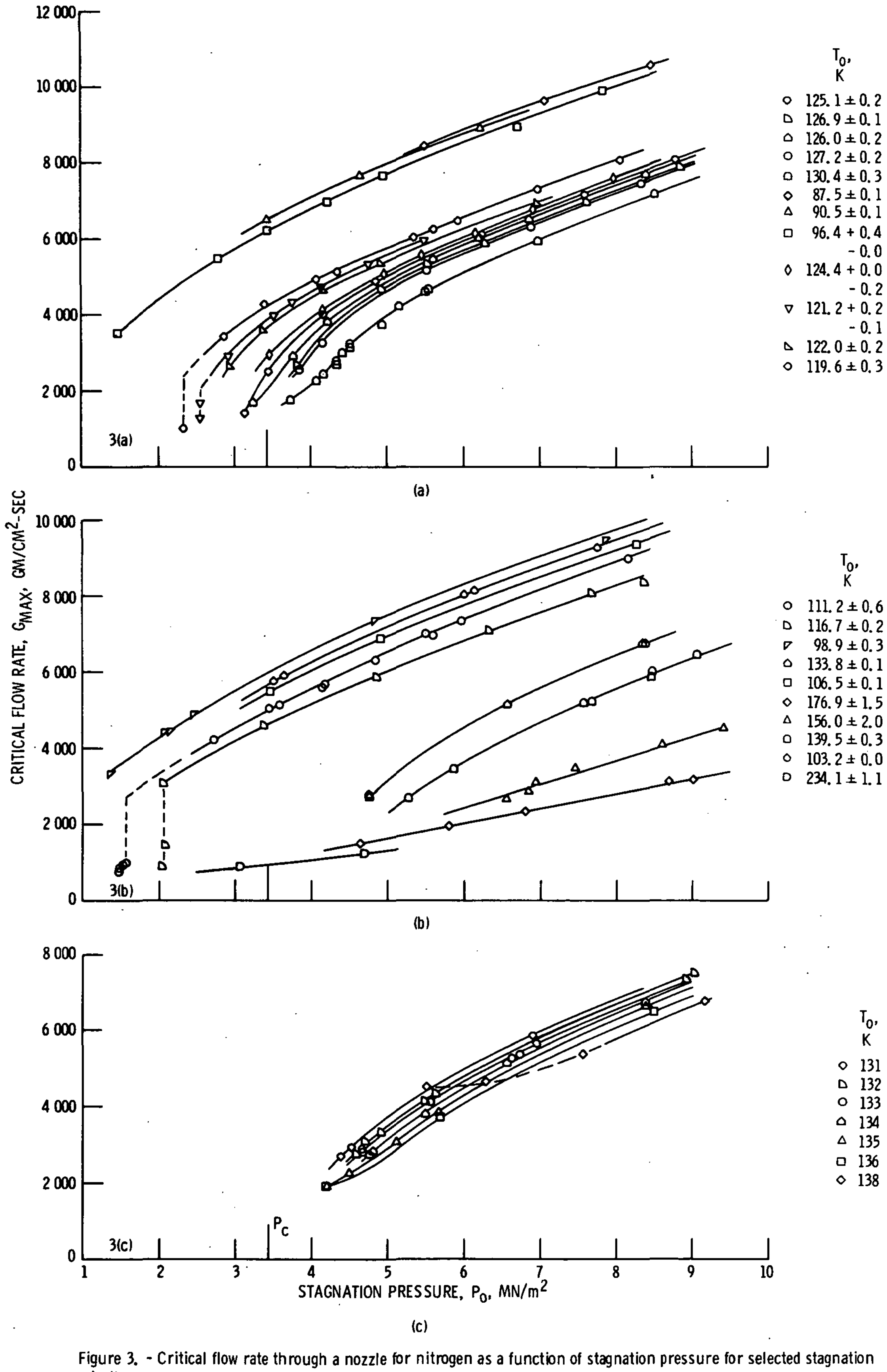

Figure 3. - Critical flow rate through a nozzle for nitrogen as a function of stagnation pressure for selected stagnation isotherms.

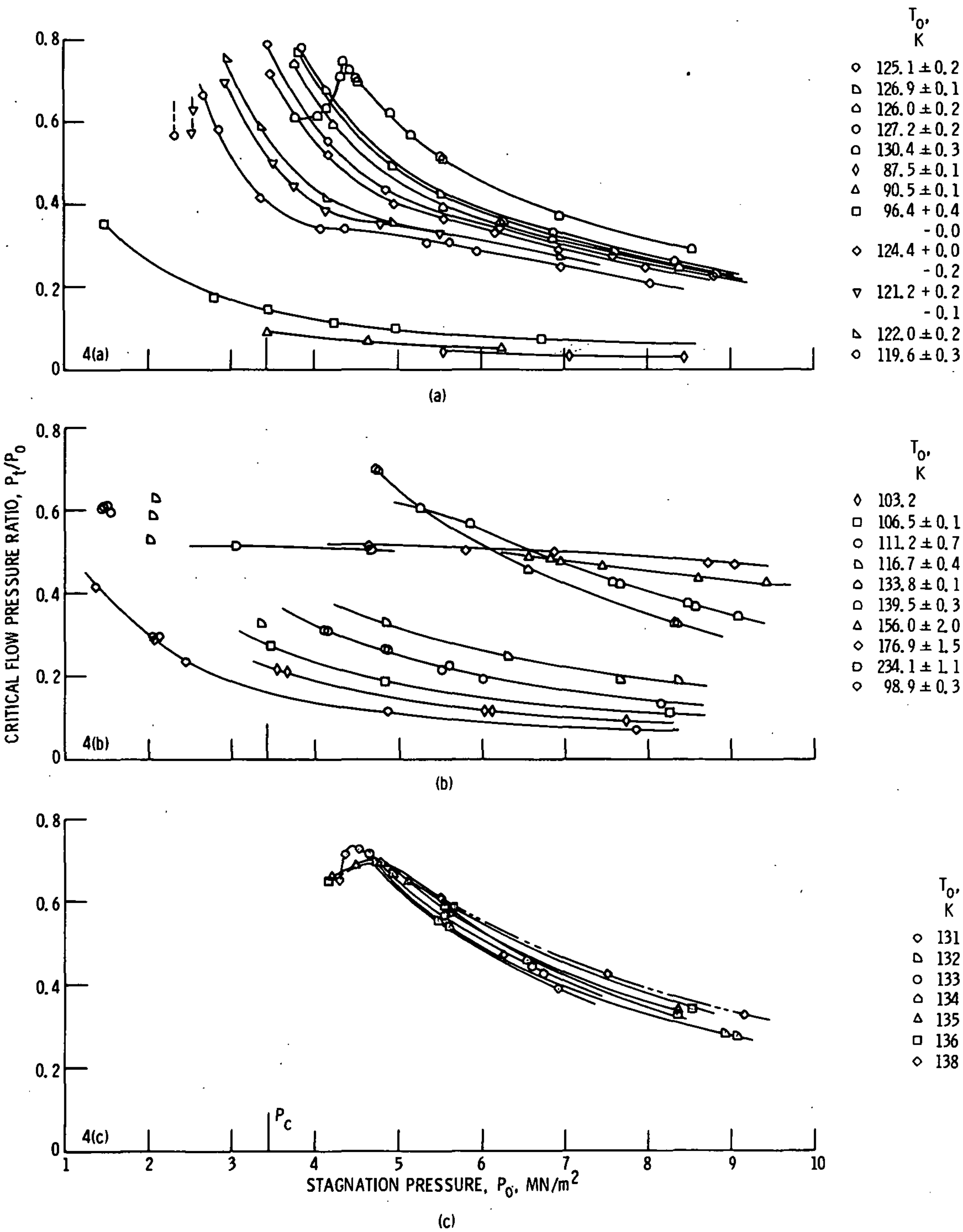

Figure 4. - Critical flow pressure ratio for nitrogen in nozzles as a function of stagnation pressure for selected stagnation isotherms.

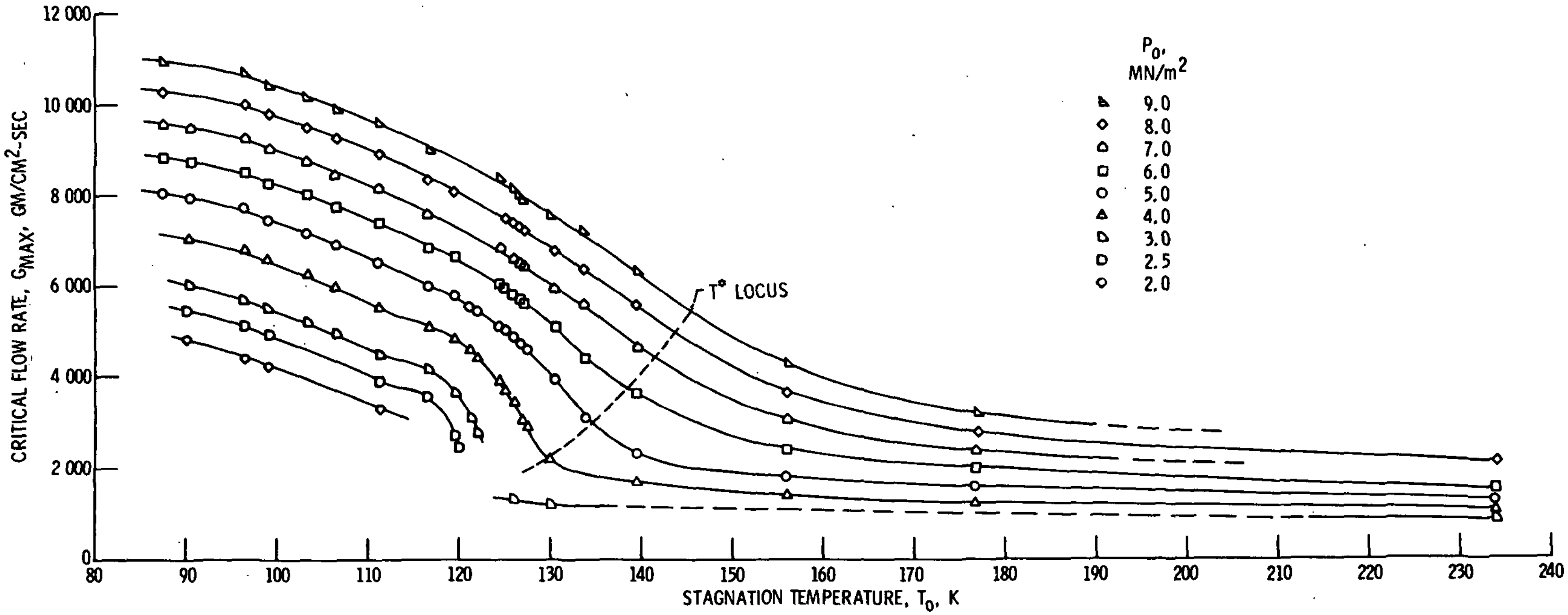

Figure 5. - Critical flow rate through a nozzle for nitrogen as a function of stagnation temperature for selected interpolated isobars.

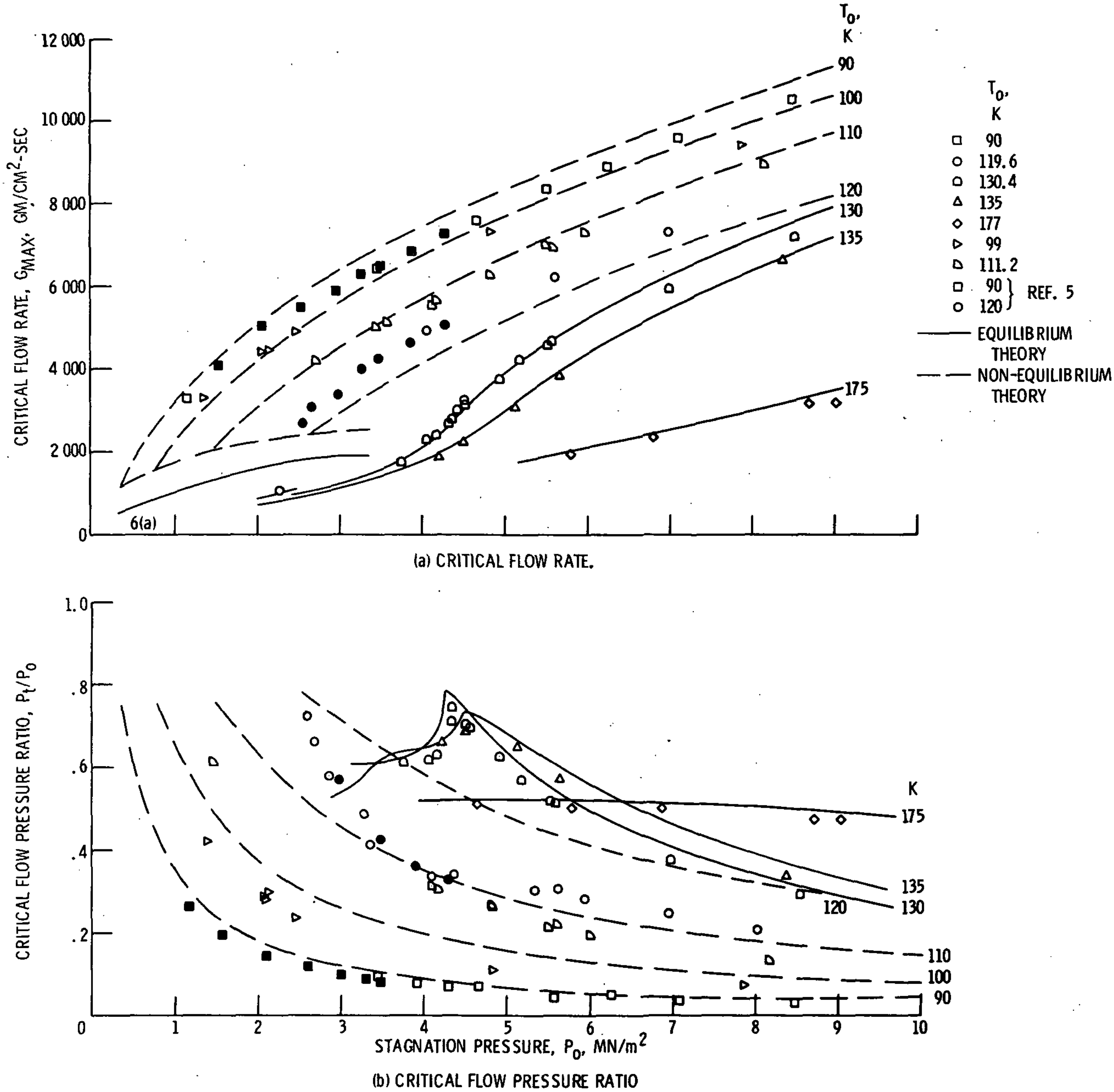

Figure 6. - Critical flow of nitrogen in nozzles. A comparison of equilibrium and two-phase theories with data $P_c = 3.417$ MN/m^2; $T_c = 126.3$ K; $\rho_c = 0.3105$ gm/cc.

E-7044

NASA-Lewis-Com'l